

Night-time chemistry above London: measurements of NO_3 and N_2O_5 from the BT Tower

A. K. Benton^{1,*}, J. M. Langridge^{1,**}, S. M. Ball², W. J. Bloss³, M. Dall'Osto^{3,***}, E. Nemitz⁴, R. M. Harrison³, and R. L. Jones¹

¹Centre for Atmospheric Science, Department of Chemistry, University of Cambridge, Lensfield Road, Cambridge, CB2 1EW, UK

²Department of Chemistry, University of Leicester, University Road, Leicester, LE1 7RH, UK

³National Centre for Atmospheric Science, School of Geography, Earth & Environmental Sciences, University of Birmingham, Birmingham, B15 2TT, UK

⁴Centre for Ecology and Hydrology (Edinburgh), Bush Estate, EH26 0QB, Penicuik, UK

* now at: British Antarctic Survey, Natural Environment Research Council, High Cross, Madingley Road, Cambridge, CB3 0ET, UK

** now at: Cooperative Institute for Research in Environmental Sciences (CIRES), University of Colorado at Boulder, and NOAA Earth System Research Laboratory (ESRL), Boulder, Colorado, USA

*** now at: Instituto de Diagnóstico Ambiental y Estudios del Agua (IDAEA), Consejo Superior de Investigaciones Científicas (CSIC), C/ LLuis Solé i Sabarís s/n; 08028, Barcelona, Spain

Received: 7 May 2010 – Published in Atmos. Chem. Phys. Discuss.: 9 June 2010

Revised: 11 September 2010 – Accepted: 9 October 2010 – Published: 19 October 2010

Abstract. Broadband cavity enhanced absorption spectroscopy (BBCEAS) has been used to measure the sum of concentrations of NO_3 and N_2O_5 from the BT (telecommunications) Tower 160 m above street level in central London during the REPARTEE II campaign in October and November 2007. Substantial variability was observed in these night-time nitrogen compounds: peak $\text{NO}_3+\text{N}_2\text{O}_5$ mixing ratios reached 800 pptv, whereas the mean night-time $\text{NO}_3+\text{N}_2\text{O}_5$ was approximately 30 pptv. Additionally, $[\text{NO}_3+\text{N}_2\text{O}_5]$ showed negative correlations with $[\text{NO}]$ and $[\text{NO}_2]$ and a positive correlation with $[\text{O}_3]$. Co-measurements of temperature and NO_2 from the BT Tower were used to calculate the equilibrium partitioning between NO_3 and N_2O_5 which was always found to strongly favour N_2O_5 ($\text{NO}_3/\text{N}_2\text{O}_5=0.01$ to 0.04). Two methods are used to calculate the lifetimes for NO_3 and N_2O_5 , the results being compared and discussed in terms of the implications for the night-time oxidation of nitrogen oxides and the night-time sinks for NO_y .

1 Introduction

The nitrate radical (NO_3) is amongst the most important oxidants in the nocturnal boundary layer (NBL). It is responsible for initiating the processing of a wide range of anthropogenic and biogenic emissions and in its reactivity to some VOCs can be considered the night-time analogue of the hydroxyl radical. Understanding the atmospheric cycle of NO_3 -its formation and loss pathways, spatial variability, and role in the regulation of NO_x ($=\text{NO}+\text{NO}_2$) and budgets of volatile organic compounds (VOCs) (Atkinson, 2000), is of key importance to understanding processes impacting surface ozone formation and air quality.

1.1 Chemistry of NO_3 and N_2O_5

Figure 1 shows a simplified scheme of nocturnal nitrogen oxide chemistry. NO_2 is formed from NO (Reaction R1), which has a predominant traffic source. NO_2 and O_3 react to form NO_3 , (Reaction R2). During night-time, N_2O_5 can be formed through reaction of NO_2 and NO_3 (Reaction R3) and decomposes with rate coefficient k_{-3} .



Correspondence to: A. K. Benton
(aibe@bas.ac.uk)

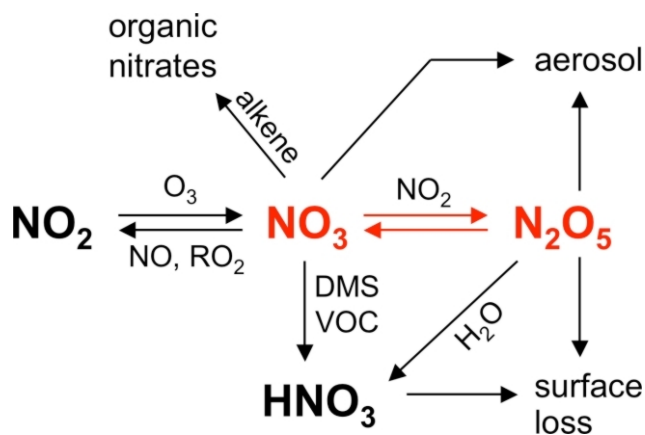
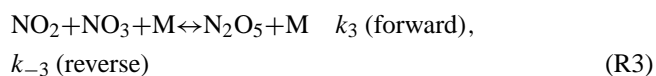
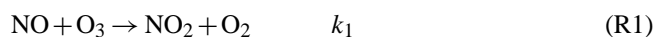


Fig. 1. Simplified schematic of nocturnal NO_y chemical processes.



At night NO₃ and N₂O₅ exist in a temperature dependent equilibrium (Wangberg et al., 1997) which is established within minutes under typical atmospheric conditions (Brown, 2003). The major sinks for NO₃ are solar photolysis (Stark et al., 2007) which effectively suppresses NO₃ and N₂O₅ concentrations during daylight hours, and the extremely fast reaction with NO (Hammer et al., 1986).

In addition to gas phase sinks, the heterogeneous conversion of N₂O₅ to aqueous nitrate (Reaction R4) provides an effective pathway for removal of NO_x from the atmosphere (Brown et al., 2004; Dentener and Crutzen, 1993).



Despite recognition of the importance of this process, its global influence remains relatively poorly quantified, in large part due to the complexity of the dependence of N₂O₅ uptake on aerosol chemical composition and mixing state (Hallquist et al., 2000; Mentel et al., 1996). Recent investigations have found that night-time removal of NO_y (=all oxides of nitrogen) via the above channels can be almost as effective at removing NO_y from the atmosphere as the major daytime pathway proceeding via the reaction of OH with NO₂ (Brown et al., 2007a, b) (Reaction R5).



1.2 Vertical extent of NO₃ and N₂O₅ structure

A number of factors lead to pronounced vertical structure of N₂O₅ and NO₃ in the NBL. NO sources are generally located

at the ground surface and act to suppress both local NO₃ and O₃ concentrations through NO₃ reacting with NO and O₃ loss (Reaction R1) leading to slower NO₃ formation (Reaction R2). Upon ascent through the atmosphere, O₃ levels increase and there is gradual conversion of NO to NO₂ followed by NO₃ and N₂O₅. The absence of significant sinks for NO₃ and N₂O₅ aloft enables significant concentrations of these species to grow, leading to distinct positive vertical concentration gradients.

Meteorological conditions also play a role in establishing vertical gradients. The absence of convection from the surface at night tends to decrease turbulent mixing and leads to a highly stratified, stable layer forming in the first few hundred metres of the NBL (Wood et al., 2010). The upper region of the NBL is therefore separated from the surface and is less affected by the surface emissions that can act to destroy NO₃.

1.3 Measurements of NO₃ and N₂O₅

Following the first detection of NO₃ in the troposphere by DOAS (Platt et al., 1980) a wide range of surface-based field studies have sought to investigate the role of NO₃ in polluted and clean air environments (e.g. Allan et al., 2000; Geyer et al., 2001; Smith et al., 1995). These studies were generally focused on NO₃ only, as N₂O₅ does not absorb at visible wavelengths, rendering it undetectable using the DOAS technique. In order to overcome this limitation, a number of NO₃ instruments have recently been developed to infer N₂O₅ concentrations through the thermal manipulation of the equilibrium between NO₃ and N₂O₅. These experiments have generally used high-finesse cavity techniques (e.g. Brown et al., 2007a; Dube et al., 2006), ionization mass spectrometry (Slusher et al., 2004) or Laser Induced Fluorescence (LIF) in-situ detectors for the NO₃ produced from thermal dissociation of N₂O₅ (Matsumoto et al., 2005b; Wood et al., 2005). Mixing ratios of up to 800 pptv of N₂O₅ were recently observed in Tokyo, Japan, using one such technique (Matsumoto et al., 2005a).

As the importance of NO₃ and N₂O₅ aloft has become apparent, a number of studies have sought to make vertically resolved measurements of NO₃ and N₂O₅ and this remains a very active area of interest (Aliwell and Jones, 1998; Brown et al., 2007a; Fish et al., 1999; Geyer and Stutz, 2004; Jones et al., 2005; Stutz et al., 2004). Brown et al. have recently reported airborne (2007a), tower (2007b), and ground based measurements (e.g. 2003b) in the USA, with more limited measurements being made by other groups over European regions (Aliwell and Jones, 1998; McFiggans et al., 2010; Penkett et al., 2007; Povey et al., 1998). Of particular note, there remain very few measurements at altitudes of 50–300 m above ground level, where airborne measurements (Brown et al., 2005) have suggested peak concentrations may exist. Given the difficulties in performing measurements aloft in urban areas, fewer still data exist on NO₃ and N₂O₅ concentrations above densely populated areas.

To this end, this paper presents in-situ, high time resolution measurements of $[\text{NO}_3+\text{N}_2\text{O}_5]$ performed using LED-based broadband cavity enhanced absorption spectroscopy (LED-BBCEAS) over a month-long period at an altitude of 160 m over central London. These measurements formed part of the second phase of the Regent's Park and Tower Experiments (REPARTEE-II). We present an overview of the measurement dataset, together with an analysis of the lifetimes of NO_3 and N_2O_5 and the importance of these species to boundary layer chemistry and removal of NO_y in this region.

2 Experimental

2.1 The measurement site

The LED-BBCEAS instrument was deployed on level 35 of the British Telecommunications tower, 160 m above ground level in central London, United Kingdom (51:31:17° N 0:08:20° W) for 28 nights between 19 October 2007 and 15 November 2007. This tower site is relatively unusual in a cityscape in that it is taller, by a factor of approximately 9 (Barlow et al., 2009) than any other building within ~ 1 km of it. This leads to minimal local turbulence effects and loss of reactive atmospheric species to surfaces in the sampling vicinity. The tower is located close to large pollution sources, for example, Marylebone Road which is one of the busiest dual carriageways in London is approximately 300 m away from the foot of the tower. In contrast, the tower is also close (~ 700 m) to Regent's Park, where local air quality conditions are thought to be representative of urban background levels. Various chemical, particulate and meteorological measurements were made during REPARTEE-II at the BT tower, in Regent's Park and on Marylebone Road, and the reader is directed to Harrison et al. (2010) for further information.

2.2 Measurement technique: LED-BBCEAS

Broadband cavity enhanced absorption spectroscopy (BBCEAS) employing light emitting diode (LED) sources was used to provide in-situ measurements of the sum of NO_3 and N_2O_5 on the BT tower. The BBCEAS technique was introduced in 2003 by Fiedler et al. (2003) and has since been developed by a number of groups (Platt et al., 2009; Ruth et al., 2007; Washenfelder et al., 2008) including the current authors (Ball et al., 2004; Langridge et al., 2006, 2008a, b). A detailed description of the BBCEAS technique and the instrument used in this study is provided in Langridge et al. (2008a) and only a brief outline is provided here.

A BBCEAS measurement is conducted by exciting a high finesse optical cavity with a broadband continuous-wave light source. The intensity transmitted through the cavity rapidly establishes a steady state level, determined principally by the input optical power, the cavity mirror reflectiv-

ity and the absorption and scattering properties of the intracavity medium. By performing spectrally resolved measurements of the transmitted cavity intensity both in the absence (I_0) and presence (I) of the absorbing gas of interest, the sample absorption coefficient can be determined from Eq. (1) (Fiedler et al., 2003), where $R(\lambda)$ is the wavelength dependent reflectivity of the mirrors used to form the cavity and d_{eff} is the effective distance between cavity mirrors, accounting for differences between the true mirror-to-mirror distance and the length over which the sample gas fills the cavity.

$$\text{Abs}(\lambda) = \left(\frac{I_0(\lambda)}{I(\lambda)} - 1 \right) \frac{1 - R(\lambda)}{d_{\text{eff}}} \quad (1)$$

where $R(\lambda)$ is the wavelength dependent reflectivity of the mirrors used to form the cavity and d_{eff} is the effective distance between cavity mirrors, accounting for differences between the true mirror-to-mirror distance and the length over which the sample gas fills the cavity.

BBCEAS provides a direct and highly sensitive means with which to determine unambiguously the concentration of an absorbing gas in-situ. High sensitivity arises as a direct result of confining the sample gas within a high finesse optical cavity, which essentially acts as an extremely effective multi-pass optical cell. By constructing the cavity with mirrors of appropriately high reflectivity (e.g. $R > 99.95\%$), optical path lengths of many kilometers can be achieved within a cell with a physical footprint of only approximately 1 m^2 . This leads to sensitivities that are routinely better than $5 \times 10^{-9} \text{ cm}^{-1}$ in 10 s (Langridge et al., 2008a). The ability of BBCEAS to determine absorber concentrations unambiguously, regardless of the presence of additional overlapping absorption features, results from the use of a broadband light source and wavelength resolved detection. Wavelength resolved spectra are captured upon every acquisition, allowing multivariate spectral fitting techniques, akin to those commonly used for differential optical absorption spectroscopy (DOAS) (Platt et al., 1980) to be used to separate contributions from molecular absorption/scattering and particulate scattering from the total extinction signal (Ball and Jones, 2009; Ball et al., 2004; Langridge et al., 2006).

One factor complicating the application of DOAS fitting principles to the analysis of BBCEAS spectra can be departure from Beer-Lambert absorption behaviour caused by strong narrow-band absorption structure, which remains unresolved by the BBCEAS measurement's limited spectral resolution. This complication is important for the analysis of BBCEAS spectra of NO_3 absorption around 662 nm (used in this work), which overlaps with strong water vapour absorption in the $4\nu + \delta$ polyad. The treatment of such complications has been described in detail by Langridge et al. (e.g. 2008a) and was applied here to analyse all ambient spectra.

2.3 LED-BBCEAS instrument

In the current work the BBCEAS instrument was operated across a wavelength range spanning 631–670 nm. This region captured the strong absorption peak of NO_3 centered at 662 nm corresponding to its $B^2E' - X^2A_2$ electronic transition, together with a significant portion of overlapping water vapour absorption structure. The instrument setup was very similar to that detailed in Langridge et al. (2008a), although operated with a slightly longer cavity length of 118.5 cm. The most important developments in this work were the use of a heated inlet to quantitatively convert ambient N_2O_5 to NO_3 and a heated cell to maintain the equilibrium in favour of NO_3 .

The inlet was constructed from PFA tubing (Adtech Ltd.) which has been shown to cause less NO_3 wall loss than alternative materials such as PTFE (Dube et al., 2006). Four individual lengths of 0.25" OD, 0.125" ID PFA tubing, each 50 cm long, were wrapped in heating tape and common insulation to form the inlet. The sample cell was constructed using 2 cm ID PFA tubing, which was also wrapped in heating tape and insulated. The inlet was joined to the sample cell at a 90° angle via a small machined PFA block employing push-fit o-ring seals. Both the inlet and sample cell were maintained at a temperature of 100 °C. A rotary pump and mass-flow controllers were used to pull air through the system at a constant flow rate of 6.8 SLPM (standard litres per minute). Assuming plug flow, residence times were 0.1 s and 2.5 s in the inlet and cell respectively. The residence time in the inlet was shown to be sufficient for >95% dissociation of N_2O_5 to NO_3 over the range conditions experienced during this deployment.

The cavity was mounted on an optical rail standing 1.4 m from the floor level (Fig. 2). The inlet was pointed towards the south-west (220°) and extended approximately 20 cm beyond a set of railings that enclosed the tower balcony.

2.4 Instrument operation

Spectra were collected using an integration time of 15 s for the duration of the project. Background spectra (I_0 in Eq. 1) were obtained by flushing the cavity with dry nitrogen at the same flow rate as used for ambient sampling. Since ambient (I) measurements were carried out in air, a correction was applied to the derived absorption coefficient to account for the small difference in Rayleigh scattering between N_2 and air. Collection of I_0 spectra was not fully automated during this deployment and the frequency with which they were acquired was determined, in large part, by the availability of access to the BT tower building. The intervals between I_0 spectra ranged from as short as 30 min to periods of several days. A typical deterioration in reflectivity over a period of 48 h was from a peak R (at $\lambda=660$ nm) of 0.9999 to 0.9995.

As shown in Eq. (1), the mirror reflectivity, $R(\lambda)$, is required to determine absolute absorber concentrations from

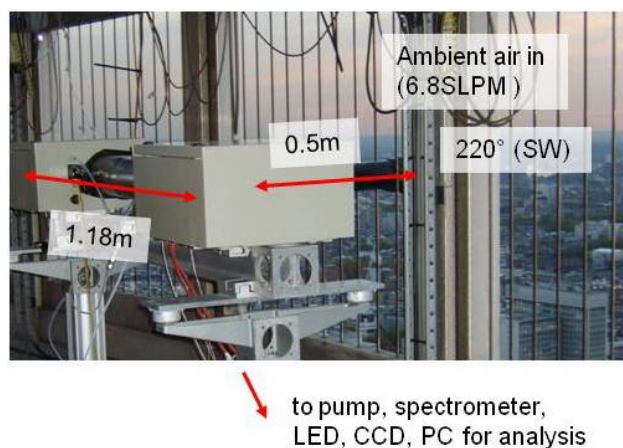


Fig. 2. The LED-BBCEAS setup on the balcony of level T35 of the BT Tower, London.

BBCEAS measurements. This quantity can change over time, for example due to dirtying of the cavity mirrors or slight changes in optical alignment caused by temperature fluctuations or mechanical movement. $R(\lambda)$ was measured periodically using phase shift cavity ringdown spectroscopy, as described by Langridge et al. (2008a). The mirror reflectivity was measured following every cavity re-alignment, mirror clean, or daily – whichever occurred most frequently, barring periods when access to the instrument was not possible for operational reasons. Calibrations of mirror reflectivity required approximately 1 hour to complete and were thus carried out during daylight hours where possible. This minimised loss of data during the night, where $[\text{NO}_3+\text{N}_2\text{O}_5]$ was most likely to be above the instrumental limit of detection (LOD).

Typically, the effective ringdown time (τ) at 660 nm of the nitrogen-flushed cavity was $25 \pm 1 \mu\text{s}$, corresponding to a reflectivity $R(\lambda)$ of 0.9999 ± 0.0001 . Figure 3 shows a set of typical spectra measured during the course of the campaign. Both the NO_3 absorption structure together with that due to water vapour are clearly visible. NO_3 mixing ratios were retrieved by differential fitting and for these examples ranged from 33 to 298 pptv.

The degradation of effective mirror reflectivity between successive phase-shift calibrations was considered. In order to quantify this degradation, the spectrally derived water concentration (see Fig. 3) was compared to water concentrations derived from relative humidity (RH) measurements made at the same level on the tower (Harrison et al., 2010). There are a number of caveats involved comparing BBCEAS-derived water concentrations with relative humidity: evaporation from aerosols can act to increase humidity; pressure needs to be accurately known in order to be able to convert RH to water concentration; and water vapour absorption spectroscopy exhibits non Beer-Lambert behaviour due to the highly structured spectral lines not being fully resolved

(Langridge, 2008; Platt and Stutz, 2008). These combined uncertainties justify not using measured and derived water mixing ratios as a primary method of mirror reflectivity calibration, but since they remain largely unchanged throughout the campaign, enable a deterioration factor to be then applied to the effective mirror reflectivity, maintaining the correlation between BBCEAS-derived humidity and that from RH measurement. This deterioration factor was never more than 0.0004%, which corresponds to a transmission efficiency reduction from 0.9998 to 0.9994 over a period of 3 days.

2.5 Uncertainty

LED-BBCEAS measurements are subject to both statistical errors, caused by uncertainty in the retrieval of spectral parameters, and systematic errors. The magnitudes of these errors are discussed here.

Statistical errors: the uncertainty in NO_3 spectral retrievals was found by determining the error in the gradient of a linear fit (Higbie, 1978) of the spectrally isolated NO_3 absorption component versus the NO_3 absorption cross section (Orphal et al., 2003). This method provides a good estimate for the measurement's LOD (Langridge, 2008). The magnitude of this uncertainty was around 2 pptv for $\text{NO}_3+\text{N}_2\text{O}_5$ for the vast majority of the campaign, but did rise for some periods to levels around 8 pptv, as shown in Fig. 4. Errors caused by changes in atmospheric pressure and uncertainties in the absorption cross section all contribute to this LOD. These increased LODs showed some correlation with periods of high aerosol extinction, which acted to limit the effective optical path length within the cavity and thus lead to poorer measurement signal-to-noise ratios, and on other occasions appeared to correlate with drifts in LED temperature which are known to affect its emission spectrum (Lee et al., 2010).

Systematic errors: the major uncertainty in the current measurements resulted from losses of reactive species to the walls of the inlet and sample cell. N_2O_5 wall losses are generally small, but those of NO_3 are significantly larger (Fuchs et al., 2008). Although ambient NO_3 generally accounted for a small part of the overall $\text{NO}_3+\text{N}_2\text{O}_5$ fraction in these studies, since almost all N_2O_5 is converted to NO_3 in the inlet of the instrument, it is important to consider the NO_3 transmission efficiency through the full system. Model calculations based on those by Bitter et al. (2005) and Fuchs et al. (2008) were used to deduce the instrument's transmission efficiency (TE) for $\text{NO}_3+\text{N}_2\text{O}_5$, taking into account the slightly different dimensions, flow rate and sample dilution in our inlet and cell. The first order wall loss coefficient for NO_3 on PFA reported by Dubé et al. of $0.2 \pm 0.05 \text{ s}^{-1}$ was used and that for the machined Teflon portion was assumed to be the same as this area accounts for less than 1% of the total surface area of the cell and inlet so any differences were deemed negligible. The total net TE was found to be $68 \pm 8\%$ but it is noted that differences in geometry between this system and that of

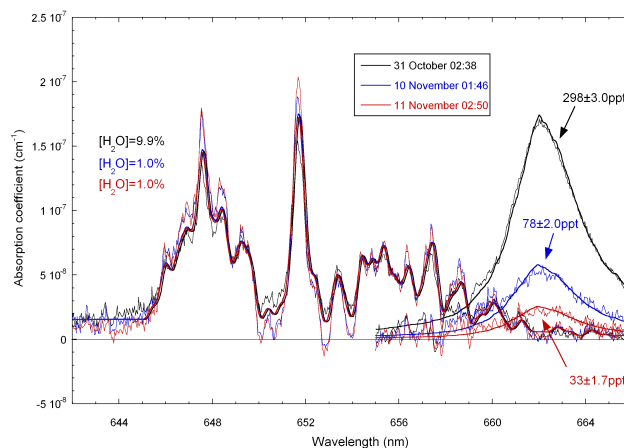


Fig. 3. Three example 15 s absorption spectra from REPARTEE-II depicting the NO_3 absorption feature at 662 nm and the polyad vibrational overtones of water vapour. Features from the same spectrum are coded by colour and dated as indicated on the plot. Derived $\text{NO}_3+\text{N}_2\text{O}_5$ mixing ratios by volume as indicated on plot take into account different mirror R values but are prior to inclusion of the inlet loss conversion factor. Absorption coefficient=0 line shown for clarity.

Dubé et al. (2006) could introduce additional unquantifiable error.

2.6 Co-measurements

NO_x measurements were carried out using a commercial NO_x analyser (Thermo TE42C-TL), employing a heated Mo catalyst for conversion of NO_2 to NO , with a temporal resolution of 1 min. A UV absorption O_3 monitor (2B-Tech Dual Beam) was also deployed (temporal resolution of 5 min), both at level T35 of the tower. Two measurements of turbulence in the vertical direction were used in this work: one from the 195 m level (mid-point of a 30 m vertical bin) of the suite of pulsed Doppler lidar (HALO Photonics, (Barlow et al., 2010) measurements; and one from an ultrasonic anemometer (S.A.) (R3-50, Gill Instruments, UK) (Barlow et al., 2010; Wood et al., 2010) situated at a height of 190 m on the top of the BT tower. A thorough discussion of vertical turbulence measurements during REPARTEE-II is detailed in Barlow et al. (2010) Furthermore, a measure of aerosol surface area (S_A) was derived using tandem (merged) Scanning Mobility Particle Sizer (SMPS) and Aerodynamic Particle Sizer (APS) measurements from level T35 of the tower (e.g. Dall'Osto et al., 2009; Shen et al., 2002). The reader is directed to the summary paper for this campaign for further information (Harrison et al., 2010).

Table 1. Statistics for night-time measurements of $[\text{NO}_3+\text{N}_2\text{O}_5]/\text{pptv}$. Night-time as defined by sunrise/sunset times. N: dataset size; 75% and 95% refers to 75th and 95th percentile; All data <LOD replaced with the median of the variable detection limit of around 2pptv and zero. Air masses grouped as indicated by a general inspection of 5-day back trajectories (Rolph, 2003) and coded by predominant origin as: P: Polar, EC: easterly continental; A: Atlantic; NC: northern continental.

Night	N	Min	25%	Median	Mean	75%	95%	Max	Air mass
19 Oct–20 Oct	4368	<LOD	<LOD	4	12	15	44	161	P
20 Oct–21 Oct	4214	<LOD	3	9	57	47	337	789	P
21 Oct–22 Oct	4093	<LOD	<LOD	<LOD	3	<LOD	11	85	NC
22 Oct–23 Oct	6872	<LOD	<LOD	11	23	29	93	390	EC
23 Oct–24 Oct	1946	<LOD	4	9	12	15	38	95	EC
24 Oct–25 Oct	2687	<LOD	<LOD	<LOD	<LOD	<LOD	<LOD	55	EC
25 Oct–26 Oct	4280	<LOD	<LOD	<LOD	<LOD	<LOD	<LOD	183	EC
29 Oct–30 Oct	207	<LOD	19	29	47	68	124	135	A
30 Oct–31 Oct	4540	<LOD	8	120	166	298	437	633	A
31 Oct–1 Nov	4307	<LOD	<LOD	<LOD	4	4	20	117	A
1 Nov–2 Nov	3977	<LOD	4	37	60	99	183	283	A
2 Nov–3 Nov	1206	<LOD	<LOD	<LOD	8	4	45	208	A
5 Nov–6 Nov	4633	<LOD	32	52	49	65	90	132	P
6 Nov–7 Nov	5131	<LOD	<LOD	12	31	45	123	237	A
7 Nov–8 Nov	4552	<LOD	9	25	32	46	92	182	A
9 Nov–10 Nov	5155	<LOD	22	43	48	70	106	197	A
10 Nov–11 Nov	5207	<LOD	14	25	28	40	59	119	A
12 Nov–13 Nov	4881	<LOD	<LOD	13	96	123	448	796	P
13 Nov–14 Nov	5260	<LOD	32	56	72	109	170	238	P
14 Nov–15 Nov	4924	<LOD	27	58	64	92	149	201	NC
All night-time data	82 453	<LOD	<LOD	16	44	52	180	796	

3 Results

LED-BBCEAS measurements commenced on 19 October 2007 at 10:00 and concluded at 09:00 on 15 November 2007 (all times UTC). The full 15 s temporal resolution dataset is shown in Fig. 4. Some spectra have been discarded due to significant misalignment of the cavity or very large increase in the retrieved LOD (a LOD value is reported for all times where analysis has been carried out but only data where $\text{NO}_3+\text{N}_2\text{O}_5 > \text{LOD}$ is shown in Fig. 4). Table 1 provides a statistical analysis of the dataset for night-periods when sufficient measurements were made. As expected, a significant diurnal trend is depicted as NO_3 is photolysed rapidly during the day and only rose above the LOD after, or within 30 min prior to sunset. A nocturnal (sunset to sunrise) mean $\text{NO}_3+\text{N}_2\text{O}_5$ mixing ratio over the whole campaign of 40 pptv was observed, with the highest nocturnal mean of 166 pptv on the night of 30–31 October 2007.

There is high variability in the temporal structure and magnitude of the observed night-time enhancements of NO_3 and N_2O_5 during this campaign. Although there were no concurrent ground-level NO_3 or N_2O_5 measurements, mixing ratios of $\text{NO}_3+\text{N}_2\text{O}_5$ measured at ground level tend to be of the order of 10 pptv (McFiggans et al., 2010), supporting the notion of a significant vertical gradient in the NBL of these

species. It is generally observed in this dataset (see Figs. 5 and 7) that any plume or injection of NO into the surrounding air corresponded to a very rapid extinction of NO_3 and N_2O_5 , suggesting that NO_3 and N_2O_5 mixing ratios are highly dependent on their source strength and therefore the titration of NO against O_3 and the very rapid reaction of NO_3 with NO to form NO_2 . This is demonstrated by the very strong negative correlation of NO_3 with NO at night (Fig. 8). This is discussed further by examination of a case study period in Sect. 3.1.

3.1 Case study period: 30 October–1 November 2007

Figure 5 shows a detailed time series covering different chemical regimes of interest of $\text{NO}_3+\text{N}_2\text{O}_5$, O_3 , (top panel) and NO, NO_2 (middle panel). The lower panel of Fig. 5 depicts two measurements of the variance of the vertical wind speed, σ_w^2 ($\text{m}^2 \text{s}^{-2}$) which is a measure of vertical turbulence and hence, an indicator of the stability of the boundary layer. Under stable conditions, vertical turbulence will be reduced, whereas under unstable conditions turbulence is higher, such as during the daytime when warming of the surface causes convection.

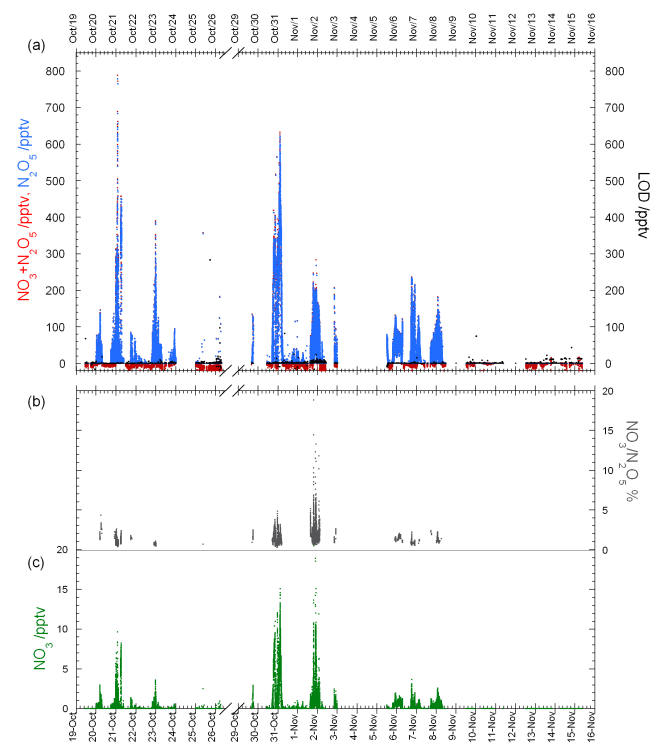


Fig. 4. LED-BBCEAS measurements of mixing ratios of $\text{NO}_3+\text{N}_2\text{O}_5$ (a, red) from the REPARTEE-II campaign. All raw data (15 s acquisitions) shown. A quantifiable measurement exists for all times where a LOD (a, black) is shown. Data partitioned into N_2O_5 (a, blue) and NO_3 (c, green) where required ancillary data (NO_2 and ambient temperature) is available. (b) (grey) shows $\text{NO}_3/\text{N}_2\text{O}_5$ ratio in %.

The first night depicted (30–31 October) illustrates a strong anti correlation of $\text{NO}_3+\text{N}_2\text{O}_5$ with NO and a positive correlation with O_3 . However, this correlation breaks down at approximately 04:30 on 31 October, when O_3 mixing ratios remain moderately high (approximately 10 ppb), but there is a sudden apparent extinction of $\text{NO}_3+\text{N}_2\text{O}_5$ indicating a change to $\text{NO}_3+\text{N}_2\text{O}_5$ sinks. Of additional interest are the periods when the instrument was performing well but NO_3 and N_2O_5 levels were near or below this LOD. On some occasions, this appears to be due to a reduced NO_3 source as NO has titrated all available O_3 (for example sunset until 22:00 on 31 October). On other occasions, (for example ~02:00 to ~06:00 on 1 November), O_3 and NO_2 are both present, and therefore the NO_3 source remains high, yet very low mixing ratios of $\text{NO}_3+\text{N}_2\text{O}_5$ are observed. In this period, the higher turbulence observed may contribute to lower $\text{NO}_3+\text{N}_2\text{O}_5$ through reduced mixing time for N_2O_5 to form, or an increase in the rate of heterogeneous loss processes indicated by larger aerosol surface area. It is noted that the increase in turbulence is accompanied by an uplift in NO and therefore an increase in NO at the tower height. However, in this instance this is not accompanied by a significant decrease

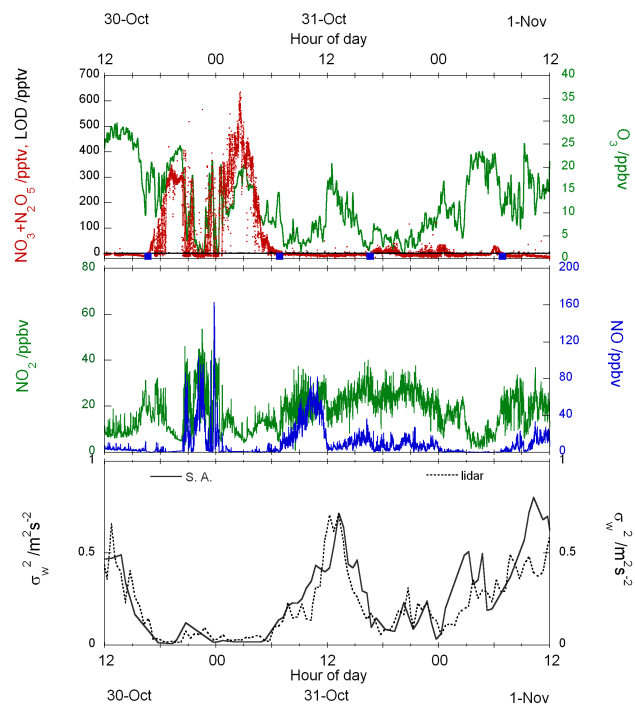


Fig. 5. A detailed plot of the continuous dataset of chemical and physical observations from 12:00 (noon) on 30 October to 12:00 on 1 November 2007. The top panel shows mixing ratios of $\text{NO}_3+\text{N}_2\text{O}_5$ (red), the LOD ~2pptv (black), (temporal resolution=15 s), O_3 mixing ratios (green) (temporal resolution=5 min) and approximate sunrise and sunset (blue squares). The middle panel shows mixing ratios of NO (blue) and NO_2 (green), (temporal resolution=1 min). The bottom panel shows the variance of w (σ_w^2), (temporal resolution=1 h) the vertical velocity component, as measured by the Doppler lidar and ultrasonic anemometer on the BT tower (see text for measurement details).

in O_3 and is not thought to therefore directly affect NO_3 production. The small increase in σ_w^2 prior to sunrise (approximately indicated by the 2nd blue square from the left in the top panel of Fig. 5), supports the hypothesis that under conditions of low turbulence, mixing ratios of $\text{NO}_3+\text{N}_2\text{O}_5$ are likely to be greater as there is less potential for deposition.

3.2 Partitioning of the NO_3 and N_2O_5 equilibrium

Where NO_2 and temperature data were available, the measured $\text{NO}_3+\text{N}_2\text{O}_5$ was partitioned into calculated ambient NO_3 and N_2O_5 concentrations assuming equilibrium conditions. The equilibrium partitioning of NO_3 and N_2O_5 can be calculated from the known (temperature dependent) equilibrium constant for Reaction (R3), provided, as is the case here, $[\text{NO}_2]$ (where a chemical species in square brackets is the number density concentration of that species) and temperature are known.

$$\frac{[\text{NO}_3]}{[\text{N}_2\text{O}_5]} = \frac{1}{K_{\text{eq}}(T)[\text{NO}_2]} \quad (2)$$

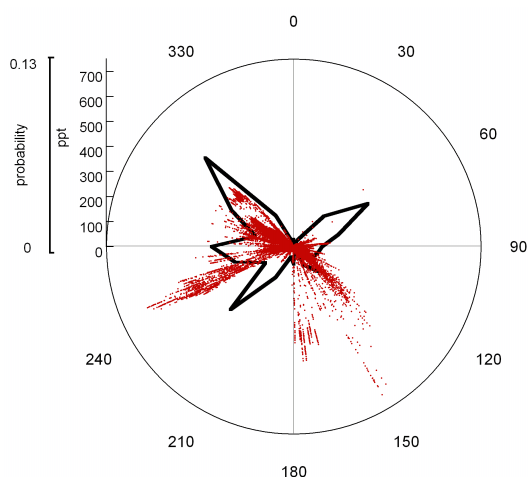


Fig. 6. Wind direction (by origin) plot of $\text{NO}_3+\text{N}_2\text{O}_5$ (hourly mean) with wind direction probability, binned into 20° regions by origin (black line), during times when BBCEAS measurements were made and an LOD reported during REPARTEE-II.

The justification for assuming that N_2O_5 is in equilibrium with NO_3 and NO_2 , tested by calculating the time for a chemical system to relax to equilibrium (τ_{eq}), (e.g. Crowley et al., 2010).

$$\tau_{\text{eq}} = \frac{1}{k_{\text{R3}}[\text{NO}_2] + k_{\text{R3}}} \quad (3)$$

τ_{eq} was derived for the measurements described here, using the forward and reverse rate coefficients for Reaction (R3) from Sander et al. (2003) calculated for the range of encountered temperatures, pressure of 1 atm, together with measured NO_2 concentrations, to give a mean time to reach equilibrium of 2.34 ± 1.66 s. The time to reach equilibrium was never more than 1 min, justifying the use of Eq. (2), as the median time for street-level emissions to reach tower height was calculated to be approximately 50 min (Barlow et al., 2010).

The mean equilibrium constant, $K_{\text{eq}}(T)$ (Sander, 2003), derived for the ambient temperature conditions of this campaign was $3.2 \pm 1.24 \times 10^{-10}$ cm^3 molecule $^{-1}$ (Maximum: K_{eq} (285 K): 8.72×10^{-10} cm^3 molecule $^{-1}$, Minimum: K_{eq} (277 K): 1.79×10^{-10} cm^3 molecule $^{-1}$), giving a mean $\text{N}_2\text{O}_5/\text{NO}_3$ ratio over the campaign of 80. High NO_2 levels shift the equilibrium in Reaction (R3) so that almost all is N_2O_5 , the maximum NO_3 observed at 31 October 2007 at 03:01 being 15 ± 0.3 pptv with corresponding N_2O_5 at this point being around 499 ± 1.63 pptv, ($\text{NO}_2=4.3$ ppbv, $\text{O}_3 \sim 7\text{--}8$ ppbv).

The NO_2 mixing ratios for REPARTEE-II were moderately high compared with other urban measurements (e.g. Platt et al., 1980) nocturnal mean ~ 20 ppbv (see Fig. 7), although not unusual for a central London site. The emissions profile and ambient temperatures of around $3\text{--}10^\circ\text{C}$ in UK Autumn, lead to a high dominance of N_2O_5 in Re-

action (R3). Therefore, where NO_2 data is unavailable and thus the equilibrium partitioning of NO_3 and N_2O_5 cannot be determined, it is reasonable to make the assumption that $[\text{NO}_3+\text{N}_2\text{O}_5] \approx [\text{N}_2\text{O}_5]$. The NO_x analyser is likely to retrieve some fraction of NO_3 and N_2O_5 as NO_2 , but as value of $[\text{NO}_3+\text{N}_2\text{O}_5]/[\text{NO}_x]$ was found to be less than 1% for the duration of the campaign no correction was applied. Interferences from other NO_y uncliding HONO and HNO_3 were considered, leading to a maximum interference of 16% assuming NO_y and NO_2 maxima coincide. Since the effect of NO_2 on the calculation of the partitioning between NO_3 and N_2O_5 is small at the temperatures experienced during REPARTEE II, this is only likely to be significant for the very low NO_2 periods (<5 ppbv). Figure 7 shows that such periods do not ever coincide with periods of high NO_3 or N_2O_5 and for the temperature and NO_2 conditions experienced during REPARTEE-II, a change of NO_2 of the order of 5–15% would have little effect on the already very small ($\sim 2\%$) N_2O_5 conversion to NO_3 .

A useful parameter to identify, when dealing with a suite of NO_x measurements, is the fraction of NO_x that is stored in the nocturnal equilibrium between NO_3 and N_2O_5 , or $F(\text{NO}_x)$, (Reaction R3) as shown by Brown et al. (2004) and McLaren et al. (2004). Smaller values of $F(\text{NO}_x)$ can be indicative of shorter N_2O_5 or NO_3 lifetimes; shorter lifetimes suggest rapid sinks for N_2O_5 .

$$F(\text{NO}_x) = \frac{[\text{NO}_3] + 2[\text{N}_2\text{O}_5]}{[\text{NO}_2] + [\text{NO}_3] + 2[\text{N}_2\text{O}_5]} \quad (4)$$

A median value of $F(\text{NO}_x)$ for REPARTEE-II night-times is around 0.05 with a mean of only 1% (Fig. 10). This is somewhat lower than previous studies in moderately polluted MBL and aloft ($\sim 0.05\text{--}0.2$) (Brown et al., 2004; McLaren et al., 2010). Elevated mixing ratios of NO_2 also act to decrease $F(\text{NO}_x)$ as measured here.

3.3 Correlations with ancillary data

No apparent correlation of $[\text{NO}_3+\text{N}_2\text{O}_5]$ with wind direction was observed (Fig. 6), nor with air mass history from 5-day back trajectory calculations (Rolph, 2003), (Table 1) consistent with the measurement site being unbiased in terms of direction of local emissions of NO_x . No bias towards the BBCEAS instrument inlet direction (220°) was observed. Indeed, the probability distribution of wind directionality in Fig. 6 depicts that this was a common directional wind sector during REPARTEE-II, but only mixing ratios of <100 pptv for $\text{NO}_3+\text{N}_2\text{O}_5$ were measured at these times.

Figure 7 shows a summary of BBCEAS-derived components of the campaign dataset, along with some useful ancillary parameters for comparison. The maximum retrieved partitioned mixing ratios for the campaign for 1 h averages were 500 pptv for N_2O_5 and 10 pptv for NO_3 . A negative correlation of night-time $\text{NO}_3+\text{N}_2\text{O}_5$ with NO (strong) and NO_2 (weak) and a positive correlation with O_3 are depicted

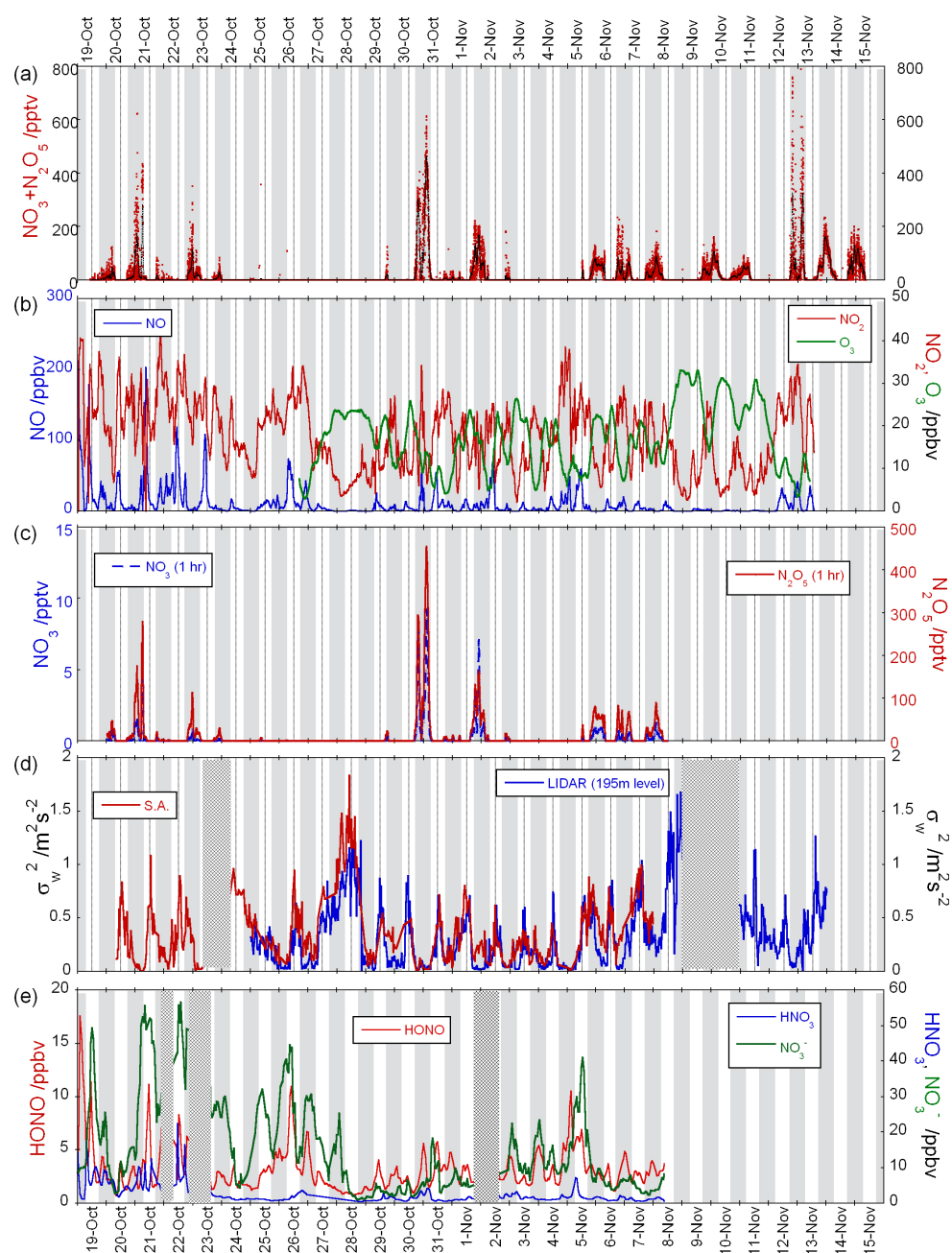


Fig. 7. A summarised time series of measurements during REPARTEE-II. **(a)** LED-BBCEAS retrieved $\text{NO}_3 + \text{N}_2\text{O}_5$ (red points), 1 h moving mean (black line). **(b)** Mixing ratios of NO, NO_2 and O_3 ; **(c)** mixing ratios of NO_3 and N_2O_5 as inferred from measurements in panels (a) and (b). Panel (c) Depicts the standard deviation of the vertical velocity variance (σ_w^2), a measure of turbulence in the vertical direction, as indicated by nearby lidar measurements (see text) at its nearest vertical level of 195m, and by the ultrasonic anemometer (S.A.) above the tower. Panel (e) shows nitrous acid (HONO), nitric acid (HNO_3) and nitrate aerosol (NO_3^-) mixing ratios for comparison. Hatched areas depict no measurement.

in Fig. 8. Panel (b) shows a direct consequence of the reaction of NO_3 with NO. The negative correlation with NO_2 is likely to be a result of an increased NO source for NO_2 production coinciding with a decrease in NO_3 , as high periods of NO will act to decrease NO_3 and increase NO_2 .

Turbulence measurements were used to indicate the meteorological regimes encountered in the NBL. The lidar is expected to slightly underestimate the vertical velocity variance compared to the sonic anemometer (Barlow et al., 2010) under more stable conditions due to the differing sampling

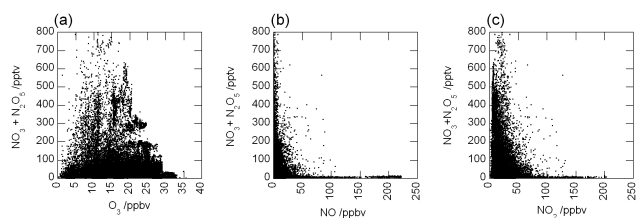


Fig. 8. Scatter plots showing correlation of mixing ratios of $\text{NO}_3+\text{N}_2\text{O}_5$ against (a) O_3 , (b) NO and (c) NO_2 for all night-time data. Data for species on horizontal axis was interpolated (within 10 minutes where available, otherwise not shown) onto same time-grid as $\text{NO}_3+\text{N}_2\text{O}_5$.

rate (4 s compared to 20 Hz respectively), this divergence is more apparent in Fig. 7. Figure 9 shows that $[\text{NO}_3+\text{N}_2\text{O}_5]$ is proportional to the inverse of both the mean night-time and maximum night-time σ_w^2 . This supports the theory that night-time $[\text{NO}_3+\text{N}_2\text{O}_5]$ enhancements occur when conditions are stable, turbulence is suppressed, and the BT tower measurements are somewhat decoupled from emissions from the surface.

3.4 Calculated lifetimes of NO_3 and N_2O_5

The lifetimes of NO_3 , ($\tau(\text{NO}_3)$) and N_2O_5 , ($\tau(\text{N}_2\text{O}_5)$) are useful for determining the magnitude of sources and sinks of NO_y in a particular regime. The lifetimes derived using Eqs. (5) and (6) rely on the assumption of a steady state for the production and loss of NO_3 and N_2O_5 and have been used in many previous studies to derive useful parameters regarding night-time NO_y

$$\tau(\text{NO}_3) = \frac{[\text{NO}_3]}{k_2[\text{O}_3][\text{NO}_2]} \quad (5)$$

$$\tau(\text{N}_2\text{O}_5) = \frac{[\text{N}_2\text{O}_5]}{k_2[\text{O}_3][\text{NO}_2]} \quad (6)$$

It has been shown (Brown et al., 2003a) that for conditions such as those during REPARTEE-II, where moderate to high NO_2 (mean night-time $\text{NO}_2 \sim 20$ ppbv) and low temperatures are experienced, although NO_3 and N_2O_5 are very likely to be in equilibrium (see Sect. 3.2), the time for NO_3 and/or N_2O_5 concentrations to reach a steady state with equal production and loss terms is likely to be several hours. This assumption was tested using a simple box model (not shown) and indeed, the derivatives of the NO_3 and N_2O_5 mixing ratios were found to confirm that a steady state is unlikely to be established over the period of one night. In addition, a measurement over a small volume such as that sampled by LED-BBCEAS diverges from steady state through transport and turbulence, as well as chemical effects. Therefore, a steady state approximation was considered unlikely to be appropriate for much of this study. It was therefore deemed prudent to compare calculations of both a steady state lifetime and

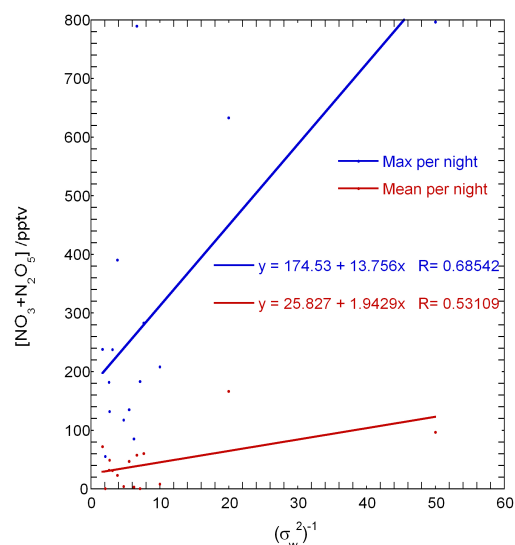


Fig. 9. Correlation plots of the reciprocal of the mean night-time standard variance of the vertical velocity (σ_w^2) against maximum (blue) and mean (red) $\text{NO}_3+\text{N}_2\text{O}_5$ mixing ratio per night during REPARTEE-II. Vertical variance data matched onto BBCEAS time-stamp. Night-time as defined by local sunrise/sunset times.

a lifetime for NO_3 and N_2O_5 taking into account the likely absence of a steady state (τ^*) as per Eq. (7) (McLaren et al., 2010).

$$\tau^*(\text{N}_2\text{O}_5 \text{ or } \text{NO}_3) = \frac{[\text{N}_2\text{O}_5 \text{ or } \text{NO}_3]}{k_2[\text{O}_3][\text{NO}_2] - \frac{d[\text{NO}_3]}{dt} - \frac{d[\text{N}_2\text{O}_5]}{dt}} \quad (7)$$

The differential of NO_3 and N_2O_5 with respect to time was calculated using a 3 point average of the 15s BBCEAS data. The result of this calculation was found to be insensitive to using larger moving averages as the measured mixing ratios were highly variable on many temporal scales. It is noted that both lifetime analyses neglect any influence of transport effects. Both determinations of τ_{ss} via Eqs. (5) and (6); and τ^* using Eq. (7) (for both NO_3 and N_2O_5) have been performed here, and in contrast to the only previous reported example of this comparison (McLaren et al., 2010), a significant difference in the results of the two methods of lifetime calculation is reported here, with the latter resulting in highly variable lifetimes, with a mean value lower by approximately 75% of its steady state counterpart. This can be seen by the diurnal trends in Fig. 10. Of particular note is that the mean lies above the 95th percentile for much of the τ^* (non-steady state) for both NO_3 and N_2O_5 lifetimes, particularly in the second half of the night, showing the highly variable nature of τ^* . This indicates that transport effects are likely to be a dominant factor influencing NO_3 and N_2O_5 mixing ratios at this site.

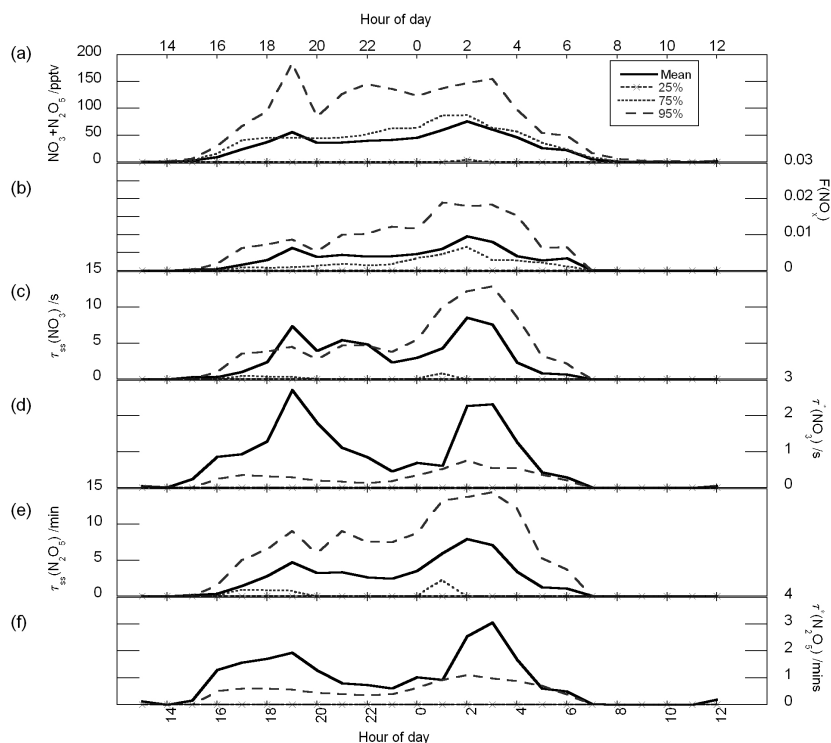


Fig. 10. Hourly average diurnal trend plots and their statistical ranges for (a) $\text{NO}_3+\text{N}_2\text{O}_5$ mixing ratios; (b) $F(\text{NO}_x)$; (c) $\tau_{\text{ss}}^*(\text{NO}_3)/\text{min}$ and (d) non steady-state $\tau^*(\text{NO}_3)/\text{s}$; (e) $\tau_{\text{ss}}^*(\text{N}_2\text{O}_5)/\text{s}$ (f) non steady-state $\tau^*(\text{N}_2\text{O}_5)/\text{min}$; for derivations of these values, see text. The large variability in both datasets is shown, as the mean being greater than the 95th percentile for much the non-steady-state treatment data. A shorter and more highly variable lifetime is determined by the non-steady state analysis.

3.5 Aerosol uptake of N_2O_5

The inability to assume a steady state under the $[\text{NO}_2]$ and typical UK autumnal temperature conditions of REPARTEE-II renders the determination of the N_2O_5 uptake coefficient, $\gamma(\text{N}_2\text{O}_5)$, difficult as many widely used determinations of k_{het} require the assumption of a steady state between NO_3 and N_2O_5 . The rate of uptake for Reaction (R4), k_{het} , was derived from Eq. (8) (Riemer et al., 2003):

$$k_{\text{het}} = \frac{1}{4} c_{\text{N}_2\text{O}_5} S_A \gamma(\text{N}_2\text{O}_5) \quad (8)$$

Here, $c_{\text{N}_2\text{O}_5}$ is the mean molecular velocity of N_2O_5 and S_A is the integrated surface area for all particles of $<1 \mu\text{m}$ diameter, (see Sect. 2.6) which takes into account the diffusion limitations to particles (Bertram and Thornton, 2009). S_A ranged from 200–1000 $\mu\text{m}^2 \text{cm}^{-2}$. The uptake coefficient, $\gamma(\text{N}_2\text{O}_5)$, was derived from a parameterisation detailed in Riemer et al. (2003) as a function of relative humidity (RH) and the ratio of mass fractions of sulphate and nitrate in aerosols (Nemitz et al., 2010a). Both the mass fraction and S_A (Fig. 11) were highly variable during the campaign. Figure 11 shows a time series of calculated k_{het} (Fig. 11), along with measured S_A and calculated $\gamma(\text{N}_2\text{O}_5)$. Mean k_{het} from these measurements was $0.17 \pm 0.08 \text{ min}^{-1}$.

The short lifetimes of N_2O_5 depicted suggest its rapid conversion to HNO_3 via Reaction (R4). Reaction of N_2O_5 with H_2O on aerosol surfaces is considered to be the principal night-time pathway for HNO_3 formation, although there is likely to be some contribution from the reaction of NO_3 with anthropogenic VOCs (such as alkenes). Assuming that each NO_3 radical goes onto form N_2O_5 and then hydrolyses to two HNO_3 molecules, the total night-integrated contribution to HNO_3 ($[\text{HNO}_3]_{\text{total}}$) from Reaction (R4) can be calculated via two methods (Wood et al., 2005).

$$[\text{HNO}_3]_{\text{total}} = 2 \int \frac{[\text{N}_2\text{O}_5]}{\tau_{\text{ss}}(\text{N}_2\text{O}_5)} dt \approx 2 \int k_2[\text{NO}_2][\text{O}_3] dt \quad (9)$$

The total integrated mixing ratio of HNO_3 was calculated for each night (sunset to sunrise) by both methods for complete nights where required ancillary datasets exist, (see Table 2) and was found to range from 2.4–11.3 ppbv via calculation using BBCEAS-inferred N_2O_5 mixing ratios and 6.6–13.5 ppbv using NO_2 and O_3 mixing ratios as measured during the campaign with the latter approach giving an average of 2 ppbv per night greater than the former. These differences serve to illustrate the shortcomings of a steady-state approximation in this instance. This difference could be due to the large calculated error in the transmission efficiency of the BBCEAS inlet potentially leading to underestimations in

Table 2. Total calculated night-time $[\text{HNO}_3]$, using $[\text{N}_2\text{O}_5]$ and $\tau_{\text{ss}}(\text{N}_2\text{O}_5)$, (2nd column); and using k_2 , $[\text{NO}_2]$ and $[\text{O}_3]$, (3rd column) of Eq. (9) for nights where a continuous dataset for all parameters were used.

Night	$[\text{HNO}_3]_{\text{a}}/\text{ppbv}$	$[\text{HNO}_3]_{\text{b}}/\text{ppbv}$
30 Oct–31 Oct	7.0 ± 1.5	8.6 ± 0.26
31 Oct–1 Nov	2.4 ± 0.50	7.0 ± 0.2
1 Nov–2 Nov	9.1 ± 1.9	10.5 ± 0.3
5 Nov–6 Nov	9.2 ± 1.9	9.8 ± 0.3
6 Nov–7 Nov	4.5 ± 1.0	6.6 ± 0.2
7 Nov–8 Nov	11.3 ± 2.4	13.5 ± 0.4

$[\text{N}_2\text{O}_5]$, but is most likely due to the approximations made in assuming a steady state for calculation of $\tau_{\text{ss}}(\text{N}_2\text{O}_5)$ (see Fig. 10), or losses other than to HNO_3 may be present, such as those involving NO_3 reactions. Aerosol surface areas, shown in Fig. 11 depict that these are not too small to be rate limiting. It should also be considered that reaction of HNO_3 with ammonia or sea salt would yield a significant aerosol concentration. Using one of the case study nights of 30–31 October, $[\text{HNO}_3]_{\text{total}}$ was calculated to be 7.0 ± 1.5 ppbv using mixing ratios of N_2O_5 and its calculated steady-state lifetime, and 8.6 ± 0.26 ppbv using NO_2 and O_3 mixing ratios which accounts for approximately $22 \mu\text{gm}^{-3}$ HNO_3 as an integrated total for this night. As the mean HNO_3 mixing ratio measurements was approximately 0.17 ppbv during this night (Nemitz et al., 2010), calculated $[\text{HNO}_3]_{\text{total}}$ represents a very small fraction of the total step-function integration of the measured mean mixing ratio, –of the order of 0.001%. HNO_3 is more likely to be formed once the air mass has travelled further from emissions sources than at this site, as longer transport and reaction times may be required for this to become a more dominant HNO_3 formation pathway.

4 Summary and conclusions

In this paper we have demonstrated the instrumental technique of LED-BBCEAS in a sustained deployment in a month-long field campaign. To our knowledge, these are the first measurements of NO_3 and N_2O_5 above a developed megacity, and give an in-situ insight into the complexity of urban nocturnal boundary layer chemistry in such a region. The instrument demonstrated the ability to measure make continuous sensitive measurements over periods long enough to perform quantitative diurnal trend analyses and produced an urban dataset useful for those wishing to test chemistry models on urban areas. A large variation in night-time concentrations was observed, with some high N_2O_5 (<800 pptv) concentrations measured. N_2O_5 appears to be very reactive and calculated lifetimes were short (of the order of minutes). In addition to nights where large enhancements are observed,

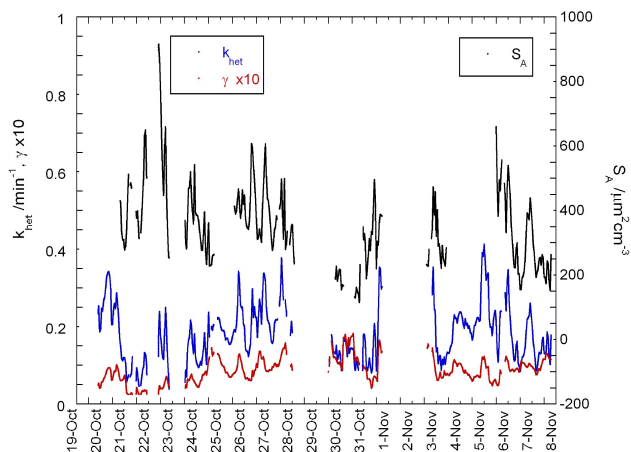


Fig. 11. Estimated parameters for the rate of uptake of N_2O_5 onto aerosols (Reaction R4). See text for details.

there were nights when the BBCEAS instrument was performing well and concentrations of N_2O_5 were below the LOD of around 2 pptv. These nights are of additional interest as they suggest an extremely large sink to source ratio, which appears to be unaccounted for by observed aerosol components. The complexity of the data rendered typical steady state analysis difficult and demonstrate the challenge of interpreting in-situ observations of short-lifetime species in a highly heterogeneous environment. The equilibrium between NO_3 and N_2O_5 was calculated from NO_2 and ambient temperature to be weighted heavily in favour of N_2O_5 and the maximum mixing ratio of NO_3 was 10 pptv averaged over 1 h. A positive correlation between the magnitude of $[\text{NO}_3 + \text{N}_2\text{O}_5]$ and $[\text{O}_3]$ was observed along with a strong negative correlation with $[\text{NO}]$ but it does not appear to be a simple function. A combination of chemical and physical sources and sinks appear to be important in determining $[\text{NO}_3]$ and $[\text{N}_2\text{O}_5]$, a theory supported by the negative correlation with a proxy for night-time turbulence. The short NO_3 and N_2O_5 lifetimes and high NO_2 conditions result in a low value of $F(\text{NO}_x)$. However, this does not necessarily mean night-time nitrate chemistry is negligible, rather that the sinks for N_2O_5 may be very rapid, leading to a potential source of nitrate in aerosols. Departures from the NO_3 N_2O_5 equilibrium do not appear to be significant, though the high NO_2 and low temperatures slow the system's approach to a steady-state. A comparison between steady state and non-steady state analyses of the lifetimes of N_2O_5 and NO_3 was performed and it was found that the system was unlikely to be in steady state, rendering steady state analysis of heterogeneous loss of N_2O_5 difficult. Estimates of the heterogeneous uptake of N_2O_5 suggest a small contribution of around 8 ppbv per night of HNO_3 via this route and suggest that potential alternate pathways for significant losses of NO_3 or N_2O_5 exist, perhaps through aerosol formation. These results demonstrate the complexity of small scale NBL

chemical processes and how they may contribute to NO_y loss budgets.

Acknowledgements. The authors thank J. F. Barlow; T. M. Dunbar, and C. R. Wood, University of Reading and F. Davies, University of Salford for access to the Doppler lidar and sonic anemometer measurements. Lidar data courtesy of the NCAS Facility for Ground-based Atmospheric Measurement (FGAM). Thanks to D. Beddows, University of Birmingham and all REPARTEE co-workers for helpful discussion. We are grateful to the BOC Science Foundation for funding REPARTEE, to BT for use of the tower, and to D. E. Heard, University of Leeds for loan of the NO_x analyser. NERC Studentship awarded to A. K. Benton ref: NER/S/A/2006/14097. We thank the referees for their helpful comments.

Edited by: W. T. Sturges

References

- Aliwell, S. R. and Jones, R. L.: Measurements of tropospheric NO₃ at midlatitude, *J. Geophys. Res.-Atmos.*, 103, 5719–5727, 1998.
- Allan, B. J., McFiggans, G., Plane, J. M. C., Coe, H., and McFadyen, G. G.: The nitrate radical in the remote marine boundary layer, *J. Geophys. Res.-Atmos.*, 105, 24191–24204, 2000.
- Atkinson, R.: Atmospheric chemistry of VOCs and NO_x, *Atmos. Environ.*, 34, 2063–2101, 2000.
- Ball, S. and Jones, R.: Broadband cavity ring-down spectroscopy, in: *Cavity ring-down spectroscopy: techniques and applications*, edited by: Berden, G. and Engeln, R., Wiley-Blackwell, Oxford, xix, 57–87, 2009.
- Ball, S. M., Langridge, J. M., and Jones, R. L.: Broadband cavity enhanced absorption spectroscopy using light emitting diodes, *Chem. Phys. Lett.*, 398, 68–74, 2004.
- Barlow, J. F., Dobre, A., Smalley, R. J., Arnold, S. J., Tomlin, A. S., and Belcher, S. E.: Referencing of street-level flows measured during the DAPPLE 2004 campaign, *Atmos. Environ.*, 43, 5536–5544, doi:10.1016/j.atmosenv.2009.05.021, 2009.
- Barlow, J. F., Dunbar, T. M., Nemitz, E. G., Wood, C. R., Gallagher, M. W., Davies, F., O'Connor, E., and Harrison, R. M.: Boundary layer dynamics over London, UK, as observed using Doppler lidar, *Atmos. Chem. Phys. Discuss.*, 10, 19901–19938, doi:10.5194/acpd-10-19901-2010, 2010.
- Bertram, T. H. and Thornton, J. A.: Toward a general parameterization of N₂O₅ reactivity on aqueous particles: the competing effects of particle liquid water, nitrate and chloride, *Atmos. Chem. Phys.*, 9, 8351–8363, doi:10.5194/acp-9-8351-2009, 2009.
- Bitter, M., Ball, S. M., Povey, I. M., and Jones, R. L.: A broadband cavity ringdown spectrometer for in-situ measurements of atmospheric trace gases, *Atmos. Chem. Phys.*, 5, 2547–2560, doi:10.5194/acp-5-2547-2005, 2005.
- Brown, S. S.: Absorption spectroscopy in high-finesse cavities for atmospheric studies, *Chem. Rev.*, 103, 5219–5238, doi:10.1021/cr020645c, 2003.
- Brown, S. S., Stark, H., and Ravishankara, A. R.: Applicability of the steady state approximation to the interpretation of atmospheric observations of NO₃ and N₂O₅, *J. Geophys. Res.-Atmos.*, 108(D17), 4539, doi:10.1029/2003JD003407, 2003a.
- Brown, S. S., Stark, H., Ryerson, T. B., Williams, E. J., Nicks, D. K., Trainer, M., Fehsenfeld, F. C., and Ravishankara, A. R.: Nitrogen oxides in the nocturnal boundary layer: Simultaneous in situ measurements of NO₃, N₂O₅, NO₂, NO, and O₃, *J. Geophys. Res.-Atmos.*, 108(D9), 4299, doi:10.1029/2002JD002917, 2003b.
- Brown, S. S., Dibb, J. E., Stark, H., Aldener, M., Vozella, M., Whitlow, S., Williams, E. J., Lerner, B. M., Jakoubek, R., Middlebrook, A. M., DeGouw, J. A., Warneke, C., Goldan, P. D., Kuster, W. C., Angevine, W. M., Sueper, D. T., Quinn, P. K., Bates, T. S., Meagher, J. F., Fehsenfeld, F. C., and Ravishankara, A. R.: Nighttime removal of NO_x in the summer marine boundary layer, *Geophys. Res. Lett.*, 31(7), L07108, doi:10.1029/2004GL019412, 2004.
- Brown, S. S., Osthoff, H. D., Stark, H., Dube, W. P., Ryerson, T. B., Warneke, C., de Gouw, J. A., Wollny, A. G., Parrish, D. D., Fehsenfeld, F. C., and Ravishankara, A. R.: Aircraft observations of daytime NO₃ and N₂O₅ and their implications for tropospheric chemistry, *J. Photochem. Photobiol. a-Chem.*, 176, 270–278, 2005.
- Brown, S. S., Dubé, W. P., Osthoff, H. D., Stutz, J., Ryerson, T. B., Wollny, A. G., Brock, C. A., Warneke, C., De Gouw, J. A., Atlas, E., Neuman, J. A., Holloway, J. S., Lerner, B. M., Williams, E. J., Kuster, W. C., Goldan, P. D., Angevine, W. M., Trainer, M., Fehsenfeld, F. C., and Ravishankara, A. R.: Vertical profiles in NO₃ and N₂O₅ measured from an aircraft: Results from the NOAA P-3 and surface platforms during the New England Air Quality Study 2004, *J. Geophys. Res.-Atmos.*, 112(D22), D22304, doi:10.1029/2007jd008883, 2007a.
- Brown, S. S., Dubé, W. P., Osthoff, H. D., Wolfe, D. E., Angevine, W. M., and Ravishankara, A. R.: High resolution vertical distributions of NO₃ and N₂O₅ through the nocturnal boundary layer, *Atmos. Chem. Phys.*, 7, 139–149, doi:10.5194/acp-7-139-2007, 2007b.
- Crowley, J. N., Schuster, G., Pouvesle, N., Parchatka, U., Fischer, H., Bonn, B., Bingemer, H., and Lelieveld, J.: Nocturnal nitrogen oxides at a rural mountain-site in south-western Germany, *Atmos. Chem. Phys.*, 10, 2795–2812, doi:10.5194/acp-10-2795-2010, 2010.
- Dall'Osto, M., Harrison, R. M., Coe, H., Williams, P. I., and Allan, J. D.: Real time chemical characterization of local and regional nitrate aerosols, *Atmos. Chem. Phys.*, 9, 3709–3720, doi:10.5194/acp-9-3709-2009, 2009.
- Dentener, F. J. and Crutzen, P. J.: Reaction of N₂O₅ on Tropospheric Aerosols – Impact on the Global Distributions of NO_x, O₃, and OH, *J. Geophys. Res.-Atmos.*, 98, 7149–7163, 1993.
- Dube, W. P., Brown, S. S., Osthoff, H. D., Nunley, M. R., Ciciora, S. J., Paris, M. W., McLaughlin, R. J., and Ravishankara, A. R.: Aircraft instrument for simultaneous, in situ measurement of NO₃ and N₂O₅ via pulsed cavity ring-down spectroscopy, *Rev. Sci. Instrum.*, 77, 034101–11, doi:10.1063/1.2176058, 2006.
- Fiedler, S. E., Hese, A., and Ruth, A. A.: Incoherent broad-band cavity-enhanced absorption spectroscopy, *Chem. Phys. Lett.*, 371, 284–294, 2003.
- Fish, D. J., Shallcross, D. E., and Jones, R. L.: The vertical distribution of NO₃ in the atmospheric boundary layer, *Atmos. Environ.*, 33, 687–691, 1999.
- Fuchs, H., Dube, W. P., Ciciora, S. J., and Brown, S. S.: Determination of inlet transmission and conversion efficiencies for in situ

- measurements of the nocturnal nitrogen oxides, NO₃, N₂O₅ and NO₂, via pulsed cavity ring-down spectroscopy, *Anal. Chem.*, **80**, 6010–6017, 2008.
- Geyer, A., Alicke, B., Konrad, S., Schmitz, T., Stutz, J., and Platt, U.: Chemistry and oxidation capacity of the nitrate radical in the continental boundary layer near Berlin, *J. Geophys. Res.-Atmos.*, **106**, 8013–8025, 2001.
- Geyer, A. and Stutz, J.: Vertical profiles of NO₃, N₂O₅, O₃, and NO_x in the nocturnal boundary layer: 2. Model studies on the altitude dependence of composition and chemistry, *J. Geophys. Res.-Atmos.*, **109**(D16), D16399, doi:10.1029/2004jd005217, 2004.
- Hallquist, M., Stewart, D. J., Baker, J., and Cox, R. A.: Hydrolysis of N₂O₅ on submicron sulfuric acid aerosols, *J. Phys. Chem. A*, **104**, 3984–3990, 2000.
- Hammer, P. D., Dlugokencky, E. J., and Howard, C. J.: Kinetics of the Gas-Phase Reaction NO + NO₃ → 2NO₂, *J. Phys. Chem.*, **90**, 2491–2496, 1986.
- Higbie, J.: Uncertainty in a Least-Squares Fit, *Am. J. Phys.*, **46**, 945–945, 1978.
- Jones, R. L., Ball, S. M., and Shallcross, D. E.: Small scale structure in the atmosphere: implications for chemical composition and observational methods, *Faraday Discuss.*, **130**, 165–179, doi:10.1039/b502633b, 2005.
- Langridge, J. M., Ball, S. M., and Jones, R. L.: A compact broadband cavity enhanced absorption spectrometer for detection of atmospheric NO₂ using light emitting diodes, *Analyst*, **131**, 916–922, 2006.
- Langridge, J. M.: Development and atmospheric applications of a novel broadband cavity enhanced absorption spectrometer, Dept. of Chem., Univ. of Cambridge, Cambridge, 2008.
- Langridge, J. M., Ball, S. M., Shillings, A. J. L., and Jones, R. L.: A broadband absorption spectrometer using light emitting diodes for ultrasensitive, in situ trace gas detection, *Rev. Sci. Instrum.*, **79**(12), 165–179, doi:10.1063/1.3046282, 2008a.
- Langridge, J. M., Laurila, T., Watt, R. S., Jones, R. L., Kaminiski, C. F., and Hult, J.: Cavity enhanced absorption spectroscopy of multiple trace gas species using a supercontinuum radiation source, *Opt. Express*, **16**, 10178–10188, 2008b.
- Langridge, J. M., Gustafsson, R. J., Griffiths, P. T., Cox, R. A., Lambert, R. M., and Jones, R. L.: Solar driven nitrous acid formation on building material surfaces containing titanium dioxide: A concern for air quality in urban areas?, *Atmos. Environ.*, **43**, 5128–5131, doi:10.1016/j.atmosenv.2009.06.046, 2009.
- Lee, J. D., McFiggans, G., Allan, J. D., Baker, A. R., Ball, S. M., Benton, A. K., Carpenter, L. J., Commane, R., Finley, B. D., Evans, M., Fuentes, E., Furneaux, K., Goddard, A., Good, N., Hamilton, J. F., Heard, D. E., Herrmann, H., Hollingsworth, A., Hopkins, J. R., Ingham, T., Irwin, M., Jones, C. E., Jones, R. L., Keene, W. C., Lawler, M. J., Lehmann, S., Lewis, A. C., Long, M. S., Mahajan, A., Methven, J., Moller, S. J., Müller, K., Müller, T., Niedermeier, N., O'Doherty, S., Oetjen, H., Plane, J. M. C., Pszenny, A. A. P., Read, K. A., Saiz-Lopez, A., Saltzman, E. S., Sander, R., von Glasow, R., Whalley, L., Wiedensohler, A., and Young, D.: Reactive Halogens in the Marine Boundary Layer (RHAMBLE): the tropical North Atlantic experiments, *Atmos. Chem. Phys.*, **10**, 1031–1055, doi:10.5194/acp-10-1031-2010, 2010.
- Matsumoto, J., Imai, H., Kosugi, N., and Kajii, Y.: In situ measurement of N₂O₅ in the urban atmosphere by thermal decomposition/laser-induced fluorescence technique, *Atmos. Environ.*, **39**, 6802–6811, 2005a.
- Matsumoto, J., Kosugi, N., Imai, H., and Kajii, Y.: Development of a measurement system for nitrate radical and dinitrogen pentoxide using a thermal conversion/laser-induced fluorescence technique, *Rev. Sci. Instrum.*, **76**, 064101–11, doi:10.1063/1.1927098, 2005b.
- McFiggans, G., Bale, C. S. E., Ball, S. M., Beames, J. M., Bloss, W. J., Carpenter, L. J., Dorsey, J., Dunk, R., Flynn, M. J., Furneaux, K. L., Gallagher, M. W., Heard, D. E., Hollingsworth, A. M., Hornsby, K., Ingham, T., Jones, C. E., Jones, R. L., Kramer, L. J., Langridge, J. M., Leblanc, C., LeCrane, J.-P., Lee, J. D., Leigh, R. J., Longley, I., Mahajan, A. S., Monks, P. S., Oetjen, H., Orr-Ewing, A. J., Plane, J. M. C., Potin, P., Shillings, A. J. L., Thomas, F., von Glasow, R., Wada, R., Whalley, L. K., and Whitehead, J. D.: Iodine-mediated coastal particle formation: an overview of the Reactive Halogens in the Marine Boundary Layer (RHAMBLE) Roscoff coastal study, *Atmos. Chem. Phys.*, **10**, 2975–2999, doi:10.5194/acp-10-2975-2010, 2010.
- McLaren, R., Salmon, R. A., Liggio, J., Hayden, K. L., Anlauf, K. G., and Leaitch, W. R.: Nighttime chemistry at a rural site in the Lower Fraser Valley, *Atmos. Environ.*, **38**, 5837–5848, doi:10.1016/j.atmosenv.2004.03.074, 2004.
- McLaren, R., Wojtal, P., Majonis, D., McCourt, J., Halla, J. D., and Brook, J.: NO₃ radical measurements in a polluted marine environment: links to ozone formation, *Atmos. Chem. Phys.*, **10**, 4187–4206, doi:10.5194/acp-10-4187-2010, 2010.
- Mentel, T. F., Bleilebens, D., and Wahner, A.: A study of nighttime nitrogen oxide oxidation in a large reaction chamber – The fate of NO₂, N₂O₅, HNO₃, and O₃ at different humidities, *Atmos. Environ.*, **30**, 4007–4020, 1996.
- Nemitz, E., Phillips, G. J., Di Marco, C. F., Allan, J., Barlow, J. F., Coe, H., Thorpe, A., Dall'Osto, M., Harrison, R. M., and Williams, P. I.: Concentrations, gradients and fluxes of inorganic reactive gases and aerosol components above London, in preparation, 2010.
- Orphal, J., Fellows, C. E., and Flaud, P. M.: The visible absorption spectrum of NO₃ measured by high-resolution Fourier transform spectroscopy, *J. Geophys. Res.-Atmos.*, **108**(11), 4077, doi:10.1029/2002jd002489, 2003.
- Penkett, S. A., Burgess, R. A., Coe, H., Coll, I., Hov, O., Lindsog, A., Schmidbauer, N., Solberg, S., Roemer, M., Thijssse, T., Beck, J., and Reeves, C. E.: Evidence for large average concentrations of the nitrate radical (NO₃) in Western Europe from the HANSA hydrocarbon database, *Atmos. Environ.*, **41**, 3465–3478, 2007.
- Platt, U., Perner, D., Winer, A. M., Harris, G. W., and Pitts, J. N.: Detection of NO₃ in the Polluted Troposphere by Differential Optical-Absorption, *Geophys. Res. Lett.*, **7**, 89–92, 1980a.
- Platt, U. and Stutz, J.: Differential Optical Absorption Spectroscopy, 1 ed., *Physics of Earth and Space Environments*, Springer, Verlag, 2008.
- Platt, U., Meinen, J., Pöhler, D., and Leisner, T.: Broadband Cavity Enhanced Differential Optical Absorption Spectroscopy (CE-DOAS) – applicability and corrections, *Atmos. Meas. Tech.*, **2**, 713–723, doi:10.5194/amt-2-713-2009, 2009.
- Povey, I. M., South, A. M., de Roodenbeke, A. T., Hill, C., Freshwater, R. A., and Jones, R. L.: A broadband lidar for the measurement of tropospheric constituent profiles from the ground, *J.*

- Geophys. Res.-Atmos., 103, 3369–3380, 1998.
- Riemer, N., Vogel, H., Vogel, B., Schell, B., Ackermann, I., Kessler, C., and Hass, H.: Impact of the heterogeneous hydrolysis of N_2O_5 on chemistry and nitrate aerosol formation in the lower troposphere under photochemical conditions, *J. Geophys. Res.-Atmos.*, 108(D4), 4144, doi:10.1029/2002JD002436, 2003.
- Ruth, A. A., Orphal, J., and Fiedler, S. E.: Fourier-transform cavity-enhanced absorption spectroscopy using an incoherent broadband light source, *Appl. Optics*, 46, 3611–3616, 2007.
- Shen, S., Jaques, P. A., Zhu, Y. F., Geller, M. D., and Sioutas, C.: Evaluation of the SMPS-APS system as a continuous monitor for measuring $\text{PM}_{2.5}$, PM_{10} and coarse ($\text{PM}_{2.5-10}$) concentrations, *Atmos. Environ.*, 36, 3939–3950, 2002.
- Slusher, D. L., Huey, L. G., Tanner, D. J., Flocke, F. M., and Roberts, J. M.: A thermal dissociation-chemical ionization mass spectrometry (TD-CIMS) technique for the simultaneous measurement of peroxyacyl nitrates and dinitrogen pentoxide, *J. Geophys. Res.*, 109, D19315, doi:10.1029/2004jd004670, 2004.
- Smith, N., Plane, J. M. C., Nien, C. F., and Solomon, P. A.: Night-time Radical Chemistry in the San-Joaquin Valley, *Atmos. Environ.*, 29, 2887–2897, 1995.
- Stark, H., Lerner, B. M., Schmitt, R., Jakoubek, R., Williams, E. J., Ryerson, T. B., Sueper, D. T., Parrish, D. D., and Fehsenfeld, F. C.: Atmospheric in situ measurement of nitrate radical (NO_3) and other photolysis rates using spectroradiometry and filter radiometry, *J. Geophys. Res.-Atmos.*, 112(D10), D10S04, doi:10.1029/2006JD007578, 2007.
- Stutz, J., Alicke, B., Ackermann, R., Geyer, A., White, A., and Williams, E.: Vertical profiles of NO_3 , N_2O_5 , O_3 , and NO_x in the nocturnal boundary layer: 1. Observations during the Texas Air Quality Study 2000, *J. Geophys. Res.-Atmos.*, 109(D16), D16398, doi:10.1029/2004jd005216, 2004.
- Wangberg, I., Etzkorn, T., Barnes, I., Platt, U., and Becker, K. H.: Absolute Determination of the Temperature Behavior of the $\text{NO}_2 + \text{NO}_3 + (\text{M}) \rightleftharpoons \text{N}_2\text{O}_5 + (\text{M})$ Equilibrium, *J. Phys. Chem. A*, 101, 9694–9698, 1997.
- Washenfelder, R. A., Langford, A. O., Fuchs, H., and Brown, S. S.: Measurement of glyoxal using an incoherent broadband cavity enhanced absorption spectrometer, *Atmos. Chem. Phys.*, 8, 7779–7793, doi:10.5194/acp-8-7779-2008, 2008.
- Wood, C. R., Lacser, A., Barlow, J. F., Belcher, S. E., Nemitz, E., Helfter, C., Famulari, D., and Grimmond, C. S. B.: Turbulent Flow at 190 m Height Above London During 2006–2008: A Climatology and the Applicability of Similarity Theory, *Bound.-Lay. Meteorol.*, 137, 77–96, doi:10.1007/s10546-010-9516-x, 2010.
- Wood, E. C., Bertram, T. H., Wooldridge, P. J., and Cohen, R. C.: Measurements of N_2O_5 , NO_2 , and O_3 east of the San Francisco Bay, *Atmos. Chem. Phys.*, 5, 483–491, doi:10.5194/acp-5-483-2005, 2005.